ORGANOMETALLICS

pubs.acs.org/Organometallics Article

Synthesis, Structure, and Solution Studies of Lithiated Allylic Phosphines and Phosphine Oxides

Nimrod M. Eren, Samantha A. Orr, Christopher D. Thompson, Emily C. Border, Michael A. Stevens, and Victoria L. Blair*

Cite This: https://dx.doi.org/10.1021/acs.organomet.0c00144 Read Online

ACCESS | Metrics & More | Article Recommendations | Supporting Information

ABSTRACT: This study reports a new series of 12 α-lithiated allylic phosphines and phosphine oxides. By incorporating Lewis base donors including diethyl ether (Et_2O), tetrahydrofuran (THF), *N,N,N′,N′*-tetramethylethylenediamine (TMEDA), and *N,N,N′,N′,N″*-pentamethyldiethylenetriamine (PMDETA), nine complexes were structurally characterized by single-crystal X-ray crystallography. This includes novel dilithiated allylic phosphine **4** [$PhP\{CHCHCH_2Li(TMEDA)\}_2$] and a rare hemisolvated lithiated phosphine oxide **6** [$\{Ph_2P(O)CHC(Me)CH_2Li\}_2(TMEDA)$]. Interestingly, in the solid state, P(III) complexes take advantage of Li$-\pi$ interactions to the newly formed delocalized system, in comparison to P(V) complexes where the oxophillic nature of the lithium atom dominates. All 12 complexes were fully characterized in the solution state by multinuclear NMR spectroscopy. DFT calculations on isomers of monomeric lithiated complex **3** [$Ph_2PCHC(Me)CH_2Li(PMDETA)$] described the low energy barrier between transition steps of the subtle delocalization of the allylic chain.

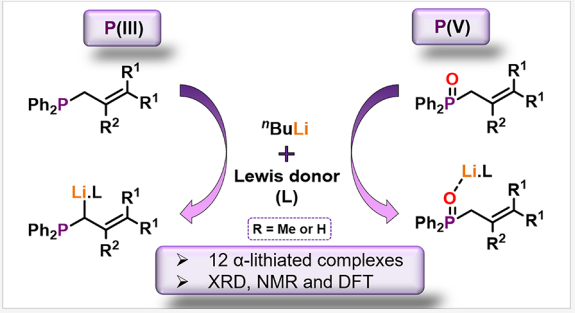

INTRODUCTION

Organophosphines are undergoing a long-awaited renaissance compared with their well-developed group 15 nitrogen analogues. To date, research efforts have focused on understanding the synthesis, reactivity, and structural chemistry, in both solid and solution states, of alkali metal amides,[1] yet the phosphine derivatives have not received as much attention.

It is well-established in the literature that phosphines are a crucial ligand class in the field of metal catalysis,[2] such as Buchwald-type dialkylbiaryl phosphine ligands[3] (Figure 1) or

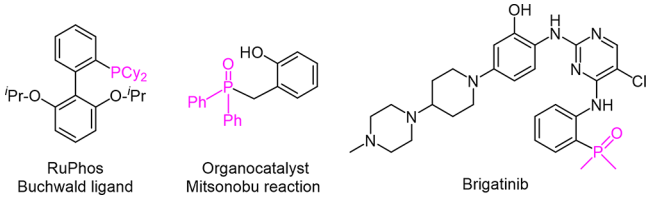

Figure 1. Examples of some prominent phosphorus containing molecules in synthetic and medicinal chemistry.

2,2′-bis(diphenylphosphino)-1,1′-binnaphthyl (BINAP) ligand employed in asymmetric synthesis,[4] while tertiary phosphines can also be employed independently as organocatalysts for various organic transformations.[5] Alongside synthetic applications, the past decade has seen the development of cyclic phosphorus compounds evolve for the use in organic electronics such as organic light-emitting diodes (OLEDs).[6] Interestingly, phosphorus-containing compounds can exhibit beneficial biological activity in medicinal chemistry.[7] In particular interest to this work is the recent FDA approval of the lung cancer drug Brigatinib[8] (Figure 1). The incorporation of a phosphine oxide functionality enhanced its desirable medicinal properties and has revived interest in understanding the importance of this functional group in medicinal chemistry. As a result of these developments, the formation of C−P bonds as a route to access novel organophosphines has been expanded,[2,9,10] while continuing to understand their structure and reactivity patterns is crucial.

In recent years, we have studied alkali metal allylic amide systems[11−13] owing to the simple building block having a significant role in accessing many valuable N-containing compounds such as β-amino acids and β-lactams,[14,15] chiral β-branched esters,[16] chiral 1,2 diamines,[17] and peptide isosteres.[18] Our ongoing interest in allylic amide systems and their applications has led us to delve into the phosphorus derivatives exploiting both oxidation states, where P(V) is air-

Received: February 28, 2020

Downloaded via UNIV OF MASSACHUSETTS AMHERST on May 26, 2020 at 18:53:41 (UTC).
See https://pubs.acs.org/sharingguidelines for options on how to legitimately share published articles.

© XXXX American Chemical Society

https://dx.doi.org/10.1021/acs.organomet.0c00144
Organometallics XXXX, XXX, XXX−XXX

stable over the P(III) analogues. Allyl phosphines have not featured extensively in the literature, although they have been incorporated into bifunctional phosphine borane FLP systems[19] and appear as donor ligands in transition metal complexes.[20,21] However, phosphine oxides feature in the literature mainly in the renowned Wittig−Horner reaction,[22−24] alongside cycloadditions,[25,26] diene synthesis,[27,28] and most recently as a superior redox-free organocatalyst for Mitsunobu reactions (Figure 1).[29]

Our group recently reported the contrasting lithiation reactivity of a N- and P-diphenylallyl system with *n*-BuLi.[30] Interestingly, notable differences were observed upon increasing the Lewis donor denticity resulting in P−C bond cleavage compared with traditional deprotonation pathways in nitrogen systems (Scheme 1). In order to extend this chemistry, the

Scheme 1. Previous Work Illustrating Lithiation of N- and P-Allyl Systems

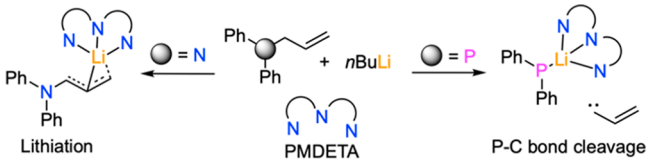

work herein focuses on understanding the lithiations of closely related substituted allyl groups including 2-methylallyl, 3,3-dimethylallyl, and diallyl phenyl phosphine compounds exploring steric and electronic influences. The analogous phosphine oxides will also be discussed and compared illustrating the impact of oxidation states on metalation patterns.

RESULTS AND DISCUSSION

Ligand Synthesis. The synthesis of P(III) allylic substrates **P1**−**P3** was achieved through an established metathesis route,[30] reacting lithium diphenyl phosphide and the corresponding allyl halide. Diallyl substrate **P4** was prepared via the Grignard reaction of phenyl phosphine dichloride with two equivalents of allyl magnesium halide (Scheme 2). All four phosphine substrates (**P1**−**P4**) were isolated as viscous colorless oils in yields ranging from 50 to 80% and fully characterized by NMR spectroscopy. The oxide derivatives

Scheme 2. Synthesis of Allylic Phenyl Phosphines and Oxides

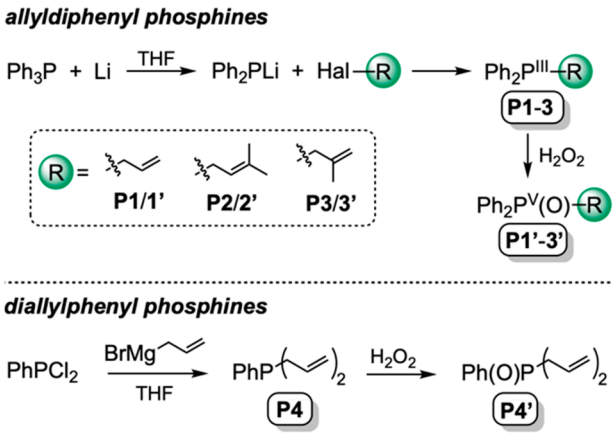

were obtained via an additional oxidation step with hydrogen peroxide to yield corresponding allylic phosphine oxides **P1′**−**P3′** as microcrystalline solids in near-quantitative yields. All four oxides where fully characterized by NMR spectroscopy and X-ray crystallography (see the Supporting Information).

Lithiation synthesis. Lithium complexes of **P2**−**P4** and **P1′**−**P3′** were synthesized by reacting the parent P-allyl substrate with *n*-BuLi at −78 °C in hexane for P(III) or diethyl ether for P(V) followed by the addition of the appropriate Lewis donor: Et_2O, THF, TMEDA, or PMDETA (Scheme 3).

Scheme 3. Summary of Lithiation of Allyl Phosphines and Oxides

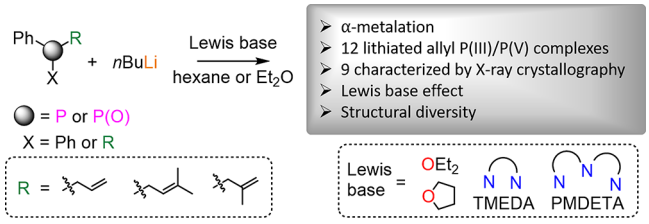

Isolation of 12 new α-lithiated complexes was achieved with nine complexes amenable to single-crystal X-ray diffraction (XRD). All complexes **1**−**12** were fully characterized by multinuclear NMR spectroscopy and microanalysis (where possible).

Structural Studies of P(III) Complexes. Single crystals suitable for XRD analysis could be obtained for four of the lithiated allyl diphenyl phosphine complexes, namely, **1** [$\{Ph_2PCHCHCMe_2Li(Et_2O)\}_2$], **2** [$\{Ph_2PCHCHCMe_2Li(TMEDA)\}_2$], **3** [$Ph_2PCHC(Me)CH_2Li(PMDETA)$], and **4** [$PhP\{CHCHCH_2Li(TMEDA)\}_2$] (Scheme 4). A summary of comparative bond lengths can be seen in Table 1.

Scheme 4. General Synthesis and Structural Diversity of Lithiated Allylic Phosphines

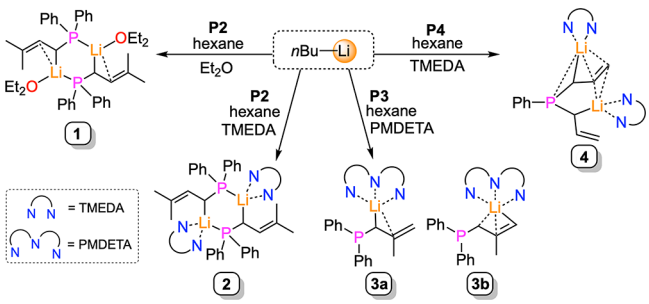

Colorless block crystals of lithiated **P2** were obtained from a hexane solution stored at −40 °C, affording α-lithiated dimer **1** [$\{Ph_2PCHCHCMe_2Li(Et_2O)\}_2$] (Figure 2). The central $(LiPC)_2$ ring core in **1** displays a distinct twist boat conformation (Figure 4) with each lithium atom formally three coordinate adopting a distorted trigonal planar olefinic carbon atom (Li1−C2, 2.250(6) Å; Li2−C7, 2.173(6) Å) increasing its coordination number to four. Notably, subtle delocalization is seen following deprotonation of the α-carbon, highlighted by contraction of the P1−C1 and C1−C2 bonds [1.752(3) and 1.434(4) Å, respectively] and elongation of the C═C bond length [1.357(4) Å]. Moving to the bidentate donor TMEDA, crystallization of lithiated **P2** from hexane and

https://dx.doi.org/10.1021/acs.organomet.0c00144
Organometallics XXXX, XXX, XXX−XXX

Table 1. Summary of Bond Lengths for Crystallographically Characterized Complexes 1−9

	P(III) complexes					P(V) complexes				
	1	2	3a	3b	4	5	6	7	8	9
bond	dimer	dimer	monomer	monomer	monomer	dimer	dimer	monomer	monomer	monomer
P1−C1−C4	1.752(3)	1.753(2)	1.7636(12)	1.7620(13)	1.797(6) 1.707(9)	1.7083(12)	1.7056(14)	1.7003(17)	1.696(2)	1.7073(16)
P1−O1						1.5240(10)	1.5190(9)	1.5123(11)	1.5197(15)	1.5226(11)
Li1−O1						1.884(2)	1.860(2)	1.804(3)	1.801(4)	1.837(3)
Li1−O1′						1.990(2)				
Li2−O1							2.043(3)			
Li1−C1	2.224(6)	2.216(4)	2.282(2)	2.494(3)	2.296(10)		2.435(2)			
−C2	2.250(6)		2.760(3)	2.412(3)	2.194(10)	2.691(3)	2.512(2)			
−C3				2.303(3)	2.335(9)	2.403(3)				
Li2−C2					2.531(10)					
−C3					2.520(11)					
−C4					2.289(11)					
−C6	2.192(6)									
−C7	2.173(6)									
C1−C2	1.434(4)	1.419(3)	1.4447(17)	1.4168(18)	1.414(8)	1.4259(16)	1.437(2)	1.433(2)	1.436(2)	1.421(2)
C4−C5					1.444(9)					
C2−C3	1.357(4)	1.354(4)	1.367(2)	1.3732(19)	1.356(8)	1.3689(16)	1.346(2)	1.361(3)	1.348(3)	1.356(2)
C5−C6					1.375(10)					

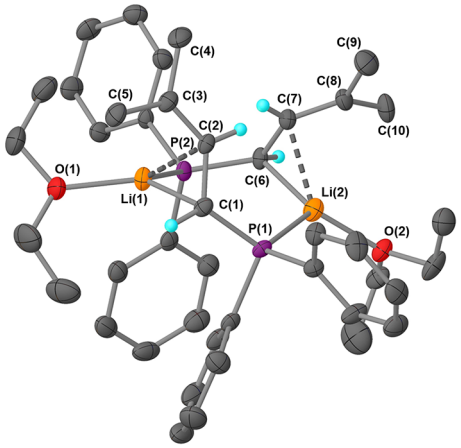

Figure 2. Molecular structure of $[\{Ph_2PCHCHCMe_2Li(Et_2O)\}_2]$ **1**. Hydrogen atoms (except allylic) are omitted for clarity. Thermal ellipsoids are shown at a 40% probability.

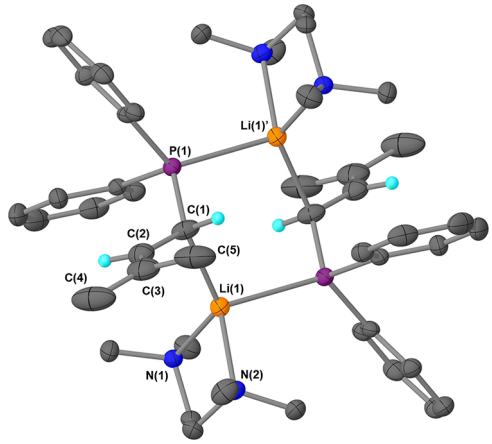

Figure 3. Molecular structure of $[\{Ph_2PCHCHCMe_2Li(TMEDA)\}_2]$ **2**. Hydrogen atoms (except allylic) are omitted for clarity. Thermal ellipsoids are shown at a 40% probability. Symmetry operator (′) = 1 − *x*, 1 − *y*, 1 − *z*.

addition of TMEDA afforded complex **2** $[\{Ph_2PCHCHCMe_2Li(TMEDA)\}_2]$ (Figure 3) in a 79% yield.

Complex **2** adopts a traditional centrosymmetric dimeric assembly with a central six-membered $(PCLi)_2$ ring assuming a chair conformation (Figure 4). Each lithium atom adopts a distorted tetrahedral geometry ($\sum$ 653.87°) with its coordination environment comprising a phosphorus atom, an α-deprotonated carbon atom [Li1−C1, 2.216(4) Å], and a bidentate chelating TMEDA molecule. Consistent with **1**, the mild delocalization of the allyl component is observed with elongated P−C and C−C bonds [1.753(2) and 1.419(3) Å, respectively], while a slight shortening of the olefinic C2−C3 bond [1.354(4) Å] is observed. Addition of bidentate TMEDA inhibits any additional Li−π electrostatic interactions, as seen in ether solvated **1**. Overall, the bonding parameters of **2** are in agreement with the reported TMEDA solvated lithiophosphine $[\{Ph_2PCH_2Li(TMEDA)\}_2]$.[31]

Moving on to phosphine **P3**, lithiation in hexane and addition of 1 equiv of PMDETA afforded a crop of single crystals identified as **3** $[Ph_2PCHC(Me)CH_2Li(PMDETA)]$.

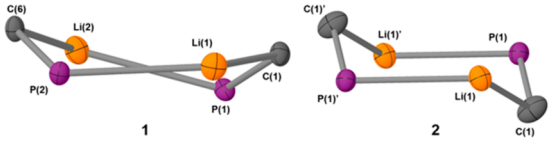

Figure 4. Comparison of $(PCLi)_2$ cores within complexes **1** and **2**.

Surprisingly, upon further inspection of the crystalline material, two distinct morphologies and crystal colors were present, namely, orange blocks **3a** and yellow blocks **3b**, both of which were suitable for XRD analysis (Figure 5). Monomeric **3a** and **3b** differ only by the interactions the lithium cation makes with the allyl component of metalated phosphine **P3**. Polymorphs **3a** and **3b** are both α-deprotonated at C1. Compound **3a** makes its shortest Li−C bond to C1 [Li1−C1 2.282(2) Å], while in isomer **3b** the lithium atom is positioned to maximize interactions with C1, C2, and C3 (average Li−C bond length 2.403 Å) with Li1−C3 displaying the shortest bond length at

https://dx.doi.org/10.1021/acs.organomet.0c00144
Organometallics XXXX, XXX, XXX−XXX

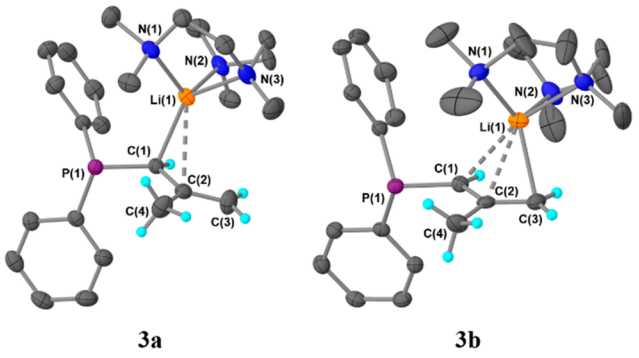

Figure 5. Molecular structures of $[Ph_2PCHC(Me)CH_2Li(PMDETA)]$ **3a** and **3b**. Hydrogen atoms (except allylic) are omitted for clarity. Thermal ellipsoids are shown at a 40% probability.

2.303(3) Å. Interestingly, despite the differing Li atom interactions on the allylic chain the C−C bond lengths in **3a** and **3b** are relatively comparable [C1−C2 1.4447(17), 1.4168(18) Å and C2−C3 1.367(2), 1.3732(19) Å, respectively]. Similar to complexes **1** and **2**, contraction of the C1−C2 bond supports moving toward a delocalized allyl chain system which is more pronounced in Li-electrostatic-rich **3b**. In contrast to our previously reported P-allylic system where PMDETA induces P−C bond cleavage,[30] here it maximizes Li-allylic electrostatic interactions to afford a stable complex.

As established in previous reported studies, nitrogen systems are well-known to form desirable aza-allyl species.[32−34] Since two isomeric forms of complex **3** were isolated in the solid state, we sought to determine the transition between **3a** and **3b**. Density functional theory (DFT) calculations were employed using the Gaussian 16[35] suite of software to help understand the cocrystallization of two isomeric forms of $[Ph_2PCHC(Me)CH_2Li(PMDETA)]$ (**3a** and **3b**) observed when using PMDETA as a ligand (Figure 6). Geometry optimization and frequency calculations were performed using the B3LYP/6-311+G(d) level and basis set which were in good agreement with the XRD structures.

Complex **3b** was found to be more stable than **3a** by ΔG = −5.6 kJ mol^{-1}, a sufficiently small difference to suggest these two structures are of comparable stability. The energy barrier between **3a** and **3b** was calculated to be marginal, ΔG = +1.5 kJ mol^{-1}. This relatively small energy difference helps explain why a mixture of products is isolated experimentally over one isomeric form. It would be reasonable to assume that the lowest energy complex, **3b**, is preferential due to the steric bulk of PMDETA, resulting in the lithium atom located further along the deprotonated allylic chain.

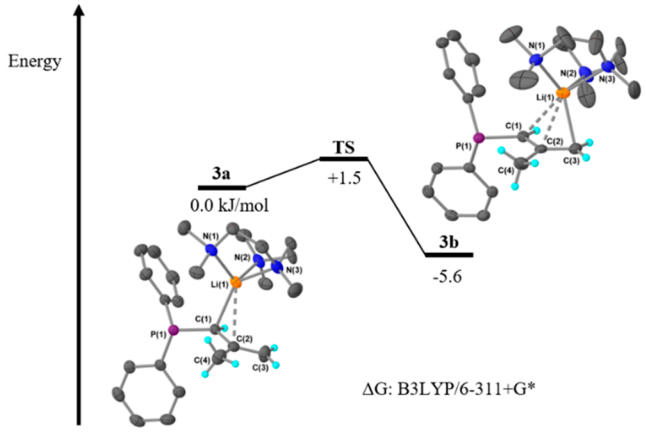

Figure 6. DFT calculations illustrating the ΔG values for the transformation between solid state isomers **3a** and **3b**.

As the phenyl ligands appear to be innocent in the structural makeup of the complex, the diallyl analogue **P4** was next investigated. **P4** was reacted with two equivalents of *n*-BuLi in hexane, which upon addition of 2 equiv of TMEDA yielded novel dilithiated diallylphenylphosphine complex **4** [PhP{$CHCHCH_2Li(TMEDA)$}$_2$] (Figure 7).

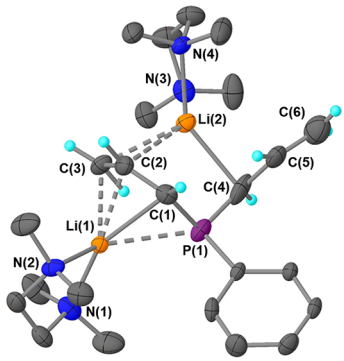

Figure 7. Molecular structure of **4** [PhP{$CHCHCH_2Li(TMEDA)$}$_2$]. Hydrogen atoms (except allylic) are omitted for clarity. Thermal ellipsoids are shown at a 40% probability.

In monomeric **4**, both allylic chains have been selectively α-deprotonated with each lithium cation solvated by one TMEDA molecule. Both lithium atoms are distinct in their coordination environments with Li1 adopting an η^4-binding mode to the P1, C1, C2, and C3 atoms on one allyl chain with the shortest Li−C bond to C2 [2.194(10) Å]. In contrast, Li2 is sandwiched between both deprotonated allylic chains making its shortest bond to α-deprotonated C4 (Li2−C4, 2.289(11) Å) and an η^2-interaction to only one of the deprotonated allylic chains via carbon atoms C2 and C3. Interestingly, despite the different electronic environments about both the deprotonated allylic chains in **4**, the C1−3 and C4−6 chain fragments are essentially equivalent in their bond lengths, with an overall contraction of the deprotonated single C1−C2 and C4−C5 bonds suggesting a dual sp^3/sp^2 nature. The cis/trans geometries of the allyl chains resonate with the bonding mode observed to the lithium cations. One notable difference in complex **4** is the asymmetric P−$C_{allylic}$ bonds [P1−C1, 1.797(6) Å; P1−C4 1.707(9) Å] in comparison to those of complexes **1**−**3** which consistently show a shortening of the P−C bond upon lithiation (avg 1.758 Å).

Structural Studies of P(V) Complexes. Upon moving to the P(V) oxidation state, a series of six new lithiated allyl phosphine oxides were isolated, of which five were characterized by XRD analysis as summarized in Scheme 5 and Table 1. Phosphine oxide **P3′** was the most successful in yielding single crystals suitable for X-ray crystallography. Lithiation of **P3′** with *n*-BuLi in diethyl ether solution and addition of THF to aid crystallization yielded a crop of orange needle crystals identified as **5** [{$Ph_2P(O)CHC(Me)CH_2Li(THF)$}$_2$] (Figure 8). The discrete centrosymmetric dimer exhibits a central four-atom $(LiO)_2$ core, reminiscent of a typical lithium alkoxide motif.[36,37] The bridging oxygen atom

https://dx.doi.org/10.1021/acs.organomet.0c00144
Organometallics XXXX, XXX, XXX−XXX

Scheme 5. General Synthesis and Structural Diversity of Lithiated Allylic Phosphine Oxides

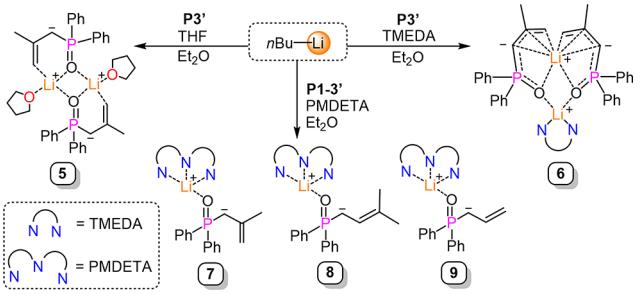

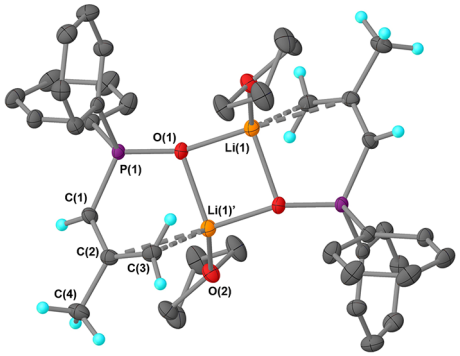

Figure 8. Molecular structure of $[\{Ph_2P(O)CHC(Me)CH_2Li(THF)\}_2]$ **5**. Hydrogen atoms (except allylic) are omitted for clarity. Thermal ellipsoids are shown at a 40% probability. Symmetry operator (′) = $-x$, $1 - y$, $1 - z$.

belonging to the phosphine oxide binds the two monomeric units together [Li1−O1 and Li1′−O1 are 1.884(2) and 1.990(2) Å, respectively], while the Li cation makes an η^2-electrostatic contact to carbon atoms C2, 2.691(3) Å, and C3, 2.403(3) Å which lie in the region of typical Li−C_{allyl} contacts.[11] The Li atoms coordination sphere is completed by a coordinating THF molecule. Overall, in the final dimeric complex the α-deprotonated allyl groups are positioned trans to each other possibly to ease steric strain.

Changing the Lewis donor to TMEDA resulted in the isolation and crystallization of rare dinuclear hemisolvated complex **6** $[\{Ph_2P(O)CHC(Me)CH_2Li\}_2(TMEDA)]$ (Figure 9). The core of **6** is composed of a $(LiO)_2$ ring in a rhombic arrangement with each lithium atom having a distinct coordination environment. The outermost lithium atom Li1 is bonded to two oxygen atoms of two α-deprotonated phosphine oxide ligands and chelated by one molecule of TMEDA in an essentially tetrahedral geometry. This appears to influence the deprotonated allyl arms into a cis arrangement encapsulating the secondary lithium cation Li2 in an η^8-fashion. The electrostatic contacts from the lithium atom Li2 to the oxygen [2.043(3) Å], phosphorus [2.6570(8) Å], and carbon [avg 2.539 Å] atoms form a stable, protective η^8-environment for the Li metal center which is persistent even upon addition of excess TMEDA. Interestingly, the bonding characteristics of the allylic chain are consistent, with shortening of the single C1−C2 bond [1.437(2) Å] and lengthening of the double C2−C3 bond [1.346(2) Å] indicating a degree of delocalization within the allylic system. Such a structural motif is unique with only limited examples observed in alkali metal chemistry. Most similar is the organophosphorous enamine complex $[\{Ph_2P(O)CH{=}C(Bu^t)N(H)Li\}_2(TMEDA)]$,[38] which exhibits a dimeric tetranuclear species in sharp contrast to the cage like motif observed in **6** emphasizing the influence of the allyl moiety in the final complex architecture.

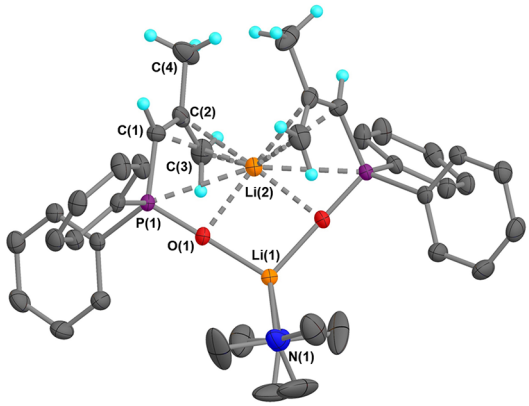

Figure 9. Molecular structure of $[\{Ph_2P(O)CHC(Me)CH_2Li\}_2(TMEDA)]$ **6**. Hydrogen atoms (except allylic) are omitted for clarity. Thermal ellipsoids are shown at a 40% probability. Symmetry operator (′) = 1 − x, + y, 3/2 −z.

Complexes **7** $[Ph_2P(O)CHC(Me)CH_2Li(PMDETA)]$, **8** $[Ph_2P(O)CHCHC(Me)_2Li(PMDETA)]$, and **9** $[Ph_2P(O)CHCHCH_2Li(PMDETA)]$ were synthesized by treating **P3′**, **P2′**, or **P1′** with 1 equiv of *n*-BuLi followed by the addition of the Lewis donor PMDETA, respectively (Scheme 5). Crystals suitable for XRD analysis of compounds **7**−**9** revealed a series of isostructural PMDETA solvated lithiated diphenyl allyl phosphine oxides. Due to their isostructural nature, only **7** has been discussed in detail (see the Supporting Information). Monomeric **7** (Figure 10) has undergone α-deprotonation

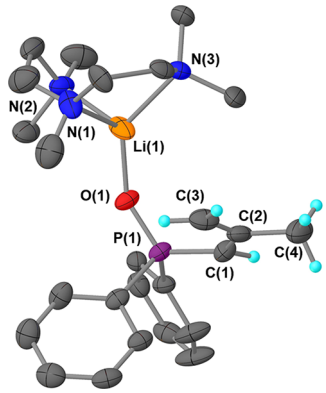

Figure 10. Molecular structure of $[Ph_2P(O)CHC(Me)CH_2Li(PMDETA)]$ **7**. Hydrogen atoms (except allylic) are omitted for clarity. Thermal ellipsoids are shown at a 40% probability.

with the lithium atom bonded to the oxygen atom of the phosphine oxide ligand [Li1−O1, 1.804(3) Å] and capped by a tridentate molecule of PMDETA. Neither the phosphorus atom nor the allyl chain display any interaction to the metal center illustrating the strong oxophillic nature of the Li cation.

Notably, there is a high degree of delocalization through the P1−C1 and P1−O1 bonds, showing considerable bond contraction (average of complexes **7**−**9** are 1.7012 and 1.5182 Å, respectively; see Table 1). This demonstrates that functionalization of the allyl chain with methyl groups at C2 or C3 does not influence the electronics of the α-deprotonated

https://dx.doi.org/10.1021/acs.organomet.0c00144
Organometallics XXXX, XXX, XXX−XXX

allyl group. However, a point of difference among the three complexes is the angle around the oxygen atom. The P1−O1−Li1 angles across **7**, **8**, and **9** are 147.03(14), 137.33(16), and 133.79(10)° where the least branched allyl chain shows the largest bond angle.

In summary, α-lithiation of the P-allylic systems result in complexes **1**−**9** exhibiting a degree of delocalization across the allyl chain fragment. This can be described as an intermediary species where the delocalization is subtle compared to nitrogen analogues where the aza-allyl nature is prominent. Interestingly, P(V) complexes **7**−**9** display additional delocalization through the P−O bond. The molecular architectures are influenced by the denticity of the Lewis base employed.

Solution-State Characterization. All 12 complexes, including three not amenable to XRD analysis, were characterized by multinuclear NMR spectroscopy (^{1}H, ^{7}Li, ^{31}P{^{1}H}, ^{13}C, COSY, and HSQC) in C_6D_6 or THF-d_8. The three additional complexes from the reaction of *n*-BuLi with parent ligands **P2**, **P3**, and **P1′** were identified as **10** [$Ph_2PCHCHCMe_2Li(PMDETA)$], **11** [$Ph_2PCHC(Me)CH_2Li(TMEDA)$], and **12** [$Ph_2P(O)CHCHCH_2Li{\cdot}Et_2O$], respectively (Scheme 6).

Scheme 6. Synthesis of Complexes 10−12

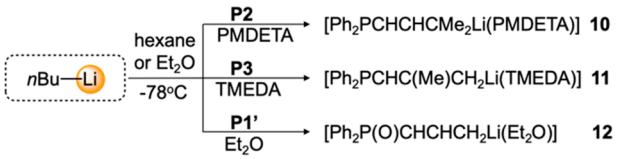

The ^{1}H NMR spectra confirm all compounds **1**−**12** have undergone selective α-lithiation, indicated by the general downfield shift of the remaining α-proton and significant downfield shift of the β-protons relative to those of the free parent phosphine or phosphine oxide (see the Supporting Information). In each complex, the corresponding donor ligand is present in the relevant ratio. The ^{7}Li NMR spectra of each complex **1**−**12** are comparable, appearing as a sharp singlet in the range of −3.73 to −5.14 ppm. Notably, the ^{31}P{^{1}H} NMR chemical shifts vary considerably across complexes **1**−**12** dependent on the coordination environment and oxidation state of the complex. This will be discussed in more detail herein.

Solution Studies P(III). In dimeric P(III) complexes **1** and **2**, which contain a direct P−Li bond, a considerable downfield shift in the ^{31}P{^{1}H} NMR signal is observed to −6.8 and −1.6 ppm, respectively (cf. parent phosphine **P2** at −15.8 ppm).

Due to the cocrystallization of monomeric isomers **3a** and **3b**, individual isolation and purification was not feasible. ^{1}H and ^{13}C NMR spectroscopic studies revealed both **3a** and **3b** exist as one species in solution, where subtle differences in their electrostatic interactions in the solid state are not observed. The ^{31}P{^{1}H} NMR resonance is less shielded appearing at −13.6 ppm compared to that of parent phosphine **P3** (cf. −17.9 ppm).

Solution studies of dilithiated complex **4** revealed that the two distinct Li cation environments in the solid state are not retained in solution with a sharp singlet at −5.14 ppm observed in the ^{7}Li NMR spectrum. In comparison, the ^{1}H NMR spectrum appears notably broad (Figure 11) which can be attributed to the fluxional nature of the allyl groups.

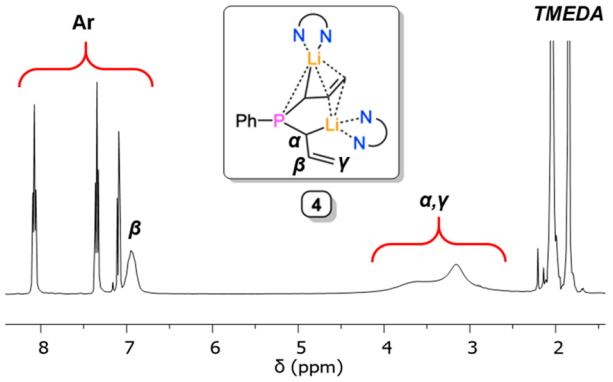

Figure 11. ^{1}H NMR spectrum of complex **4** in C_6D_6 at 25 °C.

Compound **4** is the anomaly across the P(III) complexes revealing a large upfield shift in the ^{31}P{^{1}H} NMR spectrum to −35.2 ppm (cf. parent **P4**, −26.6 ppm).

Complex **10**, which was not amenable to XRD analysis, has a ^{31}P{^{1}H} NMR spectrum chemical shift (−2.5 ppm) and a NMR profile similar to those of complexes **1** and **2**, suggesting a dimeric assembly (see the Supporting Information). In comparison, the ^{31}P{^{1}H} NMR spectrum of complex **11** in C_6D_6 is more complex, displaying three resonances at −19.7, −27.6, and −32.7 ppm. Analysis of **11** in THF-d_8 revealed a single peak at −17.4 ppm in the ^{31}P{^{1}H} NMR spectrum, suggesting the complexity and broadness of **11** in C_6D_6 could be attributed to the fluxional behavior of the allyl moiety.

Solution Studies P(V). P(V) complexes **5**−**7** possessing the same deprotonated 2-methylallyl moiety (**P3**) illustrate the influence of Lewis base donor on aggregation state. ^{1}H and ^{7}Li NMR analyses are comparable across complexes **5**−**7** with no significant differences in shift or splitting patterns observed. However, it must be noted that at room temperature in C_6D_6 compound **5** displays an extremely broad ^{1}H NMR spectrum, while the ^{31}P{^{1}H} NMR spectrum displays two broad resonances at 36.2 and 38.2 ppm, akin to the spectrum of complex **11** (see the Supporting Information). Upon performing the analysis of complex **5** in THF-d_8, the ^{1}H NMR spectrum becomes more resolved, while the ^{31}P{^{1}H} NMR spectrum displays one major resonance at 26.5 ppm in the presence of some other minor resonances (see the Supporting Information for full analysis). To confirm **5** is a single species undergoing fluxional behavior, we conducted variable-temperature studies in toluene-d_8 from 25 to 100 °C in 20 °C increments (Figure 12). As the temperature reaches 60 °C, the α- and γ-signals become resolved, while the concomitant ^{31}P{^{1}H} NMR resonances coalesce to one sharp signal at 36.8 ppm. This supports the notion that the allyl groups are displaying fluxional behavior, inducing broad spectra similar to those of complexes **4** and **11**. Post-heating analysis of the sample produced an identical spectrum to that initially collected at room temperature, ruling out a possible decomposition pathway or product.

Contrasting the ^{31}P{^{1}H} NMR profiles of **5**−**7**, they vary notably observing signals at 36.2 and 38.2 ppm (**5**), 33.3 ppm (**6**), and 26.1 ppm (**7**) upon moving from a dimer to a hemisolvated species to a monomer, where monomeric complex **7** is closest to parent phosphine **P3′** (25.9 ppm). Analogous monomeric compounds **8** and **9** have chemical shifts in a range similar to that of **7**. Comparing **7**−**9** facilitates investigating the influence of the allyl substituent, where having

https://dx.doi.org/10.1021/acs.organomet.0c00144
Organometallics XXXX, XXX, XXX−XXX

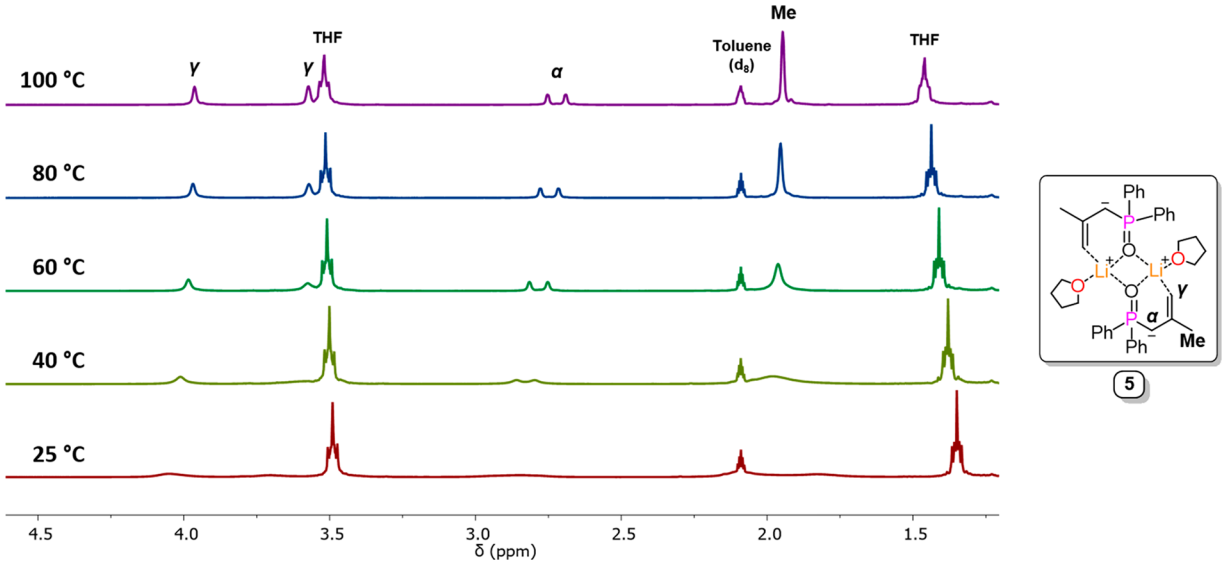

Figure 12. ^{1}H NMR spectra overlay of variable-temperature study of complex **5** in toluene-d_8.

an unbranched allyl chain (**9**) results in the most downfield shift observed in the ^{31}P{^{1}H} NMR data.

NMR analysis of **12** confirmed α-metalation with β-resonances shifting downfield relative to the resonance of the free parent phosphine oxide. The ^{31}P{^{1}H} NMR (38.8 ppm) is in line with that observed for dimeric **5** (36.2 and 38.2 ppm).

CONCLUSION

A series of α-lithiated allylic substrates have been isolated and characterized in the solid and solution states, including a novel dilithiated allylic phosphine. X-ray crystallography revealed the molecular assembly was dependent on the donor denticity, whereby the aggregation state was dimeric in the case of mono- or bidentate donors Et_2O, THF, and TMEDA but monomeric in the case of the tridentate donor PMDETA. The allylic portion of the solid-state structures, supported by DFT calculations of complexes **3a** and **3b**, displays subtle delocalization of the chain following metalation, akin to the nitrogen analogues forming aza-allylic species. Solution studies are in agreement with the solid-state structures, with delocalization of the allylic chain retained. Ongoing studies are investigating their reactivity in comparative nitrogen based cyclization pathways.

EXPERIMENTAL SECTION

All manipulations were carried under an atmosphere of argon or nitrogen using Schlenk techniques and a glovebox. Et_2O, *n*-hexane, and THF were dried and degassed using MBRAUN SPS-800 solvent purification system (SPS). Other chemicals were purchased commercially and used as received with the exception of TMEDA and PMDETA which were distilled distilled and dried over 4 Å molar sieves prior to use.

NMR Analysis. NMR spectra were recorded on a Bruker AVANCE 400 spectrometer (^{1}H, 400.13 MHz; ^{7}Li, 155.5 MHz; ^{13}C, 100.62 MHz; ^{31}P, 162.0 MHz). All ^{13}C and ^{31}P spectra were proton-decoupled. ^{1}H and ^{13}C spectra were referenced against the appropriate solvent signal. ^{7}Li and ^{31}P spectra were referenced against 9.7 M LiCl and 85% H_3PO_4 in D_2O, respectively. The proton and carbon signals were assigned by analysis of ^{1}H, ^{13}C{H}, ^{1}H−^{1}H COSY, ^{1}H−^{13}C HSQC, and ^{1}H−^{13}C HMBC.

X-ray Data. Single-crystal X-ray diffraction data were collected with a Bruker X8 APEXII CCD diffractometer with monochromatic (graphite) Mo Kα radiation processed using the Bruker Apex2 v2012.2.0 software;[39] Lorentz, polarization and absorption corrections (multiscan − SADABS)[40] were applied or a Rigaku Xtalab Synergy Dualflex diffractometer with monochromatic (graphite) Mo or Cu Kα radiation; or the MX1 synchrotron beamline at the Australian synchrotron.[41] Compounds **1**−**9** and **P1′**−**P4′** were solved and refined with SHELXT 2014/5[42] and SHELXL.[43]

Synthesis of 1 [{Ph$_2$PCHCHCMe$_2$Li(Et$_2$O)}$_2$]. 3,3-Dimethylallyldiphenylphosphine (**P2**) (0.2543 g, 1.00 mmol) was dissolved in dry *n*-hexane (10 mL). *n*-Butyllithium (0.69 mL, 1.6 M in hexane, 1.1 mmol) was then added dropwise at −78 °C, forming a yellow solution. After warming to room temperature and stirring for a further 2 h, Et_2O (0.12 mL (1.1 mmol) was added dropwise with stirring, turning the solution a brighter yellow. The solution was concentrated under reduced pressure forming a yellow-orange oil. Crystals suitable for X-ray diffraction were grown from a filtered, highly concentrated solution of hexane at −40 °C as blocks (0.087 g, 26%). ^{1}H NMR (C_6D_6, 400.20 MHz): δ 0.82 (t, $^{3}J_{H-H}$ = 7.1 Hz, 6H, Et_2O−Me), 1.90 (s, 3H, −CH═CMeMe(trans)), 2.08 (s, 3H, −CH═CMeMe(cis)), 2.61 (dd, $^{3}J_{H-H}$ = 12.7 Hz, $^{2}J_{H-P}$ = 5.1 Hz, 1H, P−CH−), 3.04 (q, $^{3}J_{H-H}$ = 7.1 Hz, 4H, Et_2O−CH_2) 6.45 (t, $^{3}J_{H-P}$ = 14.3 Hz, $^{3}J_{H-H}$ = 12.7 Hz, 1H, −CH═), 7.06 (m, 2H, *p*-H), 7.14 (m, 4H, *m*-H), 7.65 (m, 4H, *o*-H). ^{7}Li NMR (C6D6, 155.53 MHz): δ −3.73. ^{13}C NMR (C_6D_6, 100.6 MHz): δ 14.46 (s, Et_2O−CH_3), 18.93 (d, $^{4}J_{C-P}$ = 2.1 Hz, ═CMeMe(trans)), 26.57 (s, −CH═CMeMe(cis)), 34.64 (m, P−CH−), 66.29 (s, Et_2O−CH_2), 102.93 (m, ═CMe_2), 127.05 (s, *p*-C), 128.1 (m, *m*-C), 132.36 (d, $^{2}J_{C-P}$ = 14.0 Hz, *o*-C), 132.53 (m, −CH═), 146.34 (m, *i*-C). ^{31}P{H} NMR (C_6D_6, 162.0 MHz): δ −6.8. Due to the highly sensitive nature of this compound, satisfactory elemental analysis was not possible.

Synthesis of 2 [{Ph$_2$PCHCHCMe$_2$Li(TMEDA)}$_2$]. 3,3-Dimethylallyldiphenylphosphine (**P2**) (0.2543 g, 1.00 mmol) was dissolved in dry *n*-hexane (10 mL). *n*-Butyllithium (0.69 mL, 1.6 M in hexane, 1.1 mmol) was then added dropwise at −78 °C, forming yellow solution. After warming to room temperature and stirring for a further 2 h, *N*,*N*,*N*′,*N*″-tetramethylethylenediamine (TMEDA) (0.17 mL, 1.1 mmol) was added dropwise with stirring, turning the solution orange and forming an orange precipitate. The precipitate was washed with hexane (3 × 10 mL) before the remaining solvent was removed under reduced pressure with the solid isolated in an argon box (0.311 g, 79%). Crystals suitable for X-ray diffraction were grown from a room-temperature solution of hexane where stirring was stopped upon TMEDA addition as blocks. ^{1}H NMR (C_6D_6, 400.20 MHz): δ 1.46 (s, 4H, TMEDA−CH_2), 1.66 (s, 12H, TMEDA−CH_3), 1.81 (s, 3H, −CH═CMeMe(trans)), 2.01 (s, 3H, −CH═CMeMe(cis)), 2.76 (dd, $^{3}J_{H-H}$ = 12.8 Hz, $^{2}J_{H-P}$ = 7.6 Hz, 1H, P−CH−), 6.46 (ddhept, $^{3}J_{H-H}$ = 14.9 Hz, $^{3}J_{H-H}$ = 12.8 Hz, $^{4}J_{H-H}$ = 1.0 Hz, 1H, −CH═), 7.07

https://dx.doi.org/10.1021/acs.organomet.0c00144
Organometallics XXXX, XXX, XXX−XXX

(m, 2H, *p*-H), 7.19 (m, 4H, *m*-H), 7.84 (m, 4H, *o*-H). ^{7}Li NMR (C_6D_6, 155.53 MHz): δ −4.62. ^{13}C NMR (C_6D_6, 100.6 MHz): δ 18.76 (s, −CH=CMeMe(trans)), 26.49 (s, −CH=CMeMe(cis)), 42.20 (s, P−CH−), 45.28 (s, TMEDA−Me), 56.22 (s, TMEDA−CH_2), 91.63 (d, $^{3}J_{C-P}$ = 24.5 Hz, =CMe_2), 126.04 (s, *p*-C), 127.74 (m, *m*-C), 132.43 (d, $^{2}J_{C-P}$ = 17.6 Hz, *o*-C), 137.58 (d, $^{2}J_{C-P}$ = 46.3 Hz, −CH=), 150.92 (d, $^{1}J_{C-P}$ = 13.4 Hz, *i*-C). ^{31}P{H} NMR (C_6D_6, 162.0 MHz): δ −1.6. $C_{46}H_{68}Li_2N_4P_2$, (752.86): calcd C 73.38, H 9.10, N 7.44. Found C 73.39, H 9.59, N 7.29. Due to the highly sensitive nature of this compound, elemental analysis within 0.4% was not attained. A difference within 0.49% in H was the closest obtained.

Synthesis of 3 (3a and 3b) [$Ph_2PCHC(Me)CH_2Li$(PMDETA)]. 2-Methylallyldiphenylphosphine (**P3**) (0.2543 g, 1.00 mmol) was dissolved in dry *n*-hexane (10 mL). *n*-Butyllithium (0.69 mL, 1.6 M in hexane, 1.1 mmol) was then added dropwise at −78 °C, forming a slightly yellow solution with a small amount of yellow precipitate. After warming to room temperature and stirring for a further 2 h, *N*,*N*′,*N*″,*N*″-pentamethyldiethylenetriamine (PMDETA) (0.23 mL, 1.1 mmol) was added dropwise with stirring, forming more precipitate and turning the solution and precipitate orange. The precipitate was washed with hexane (3 × 10 mL) before the remaining solvent was removed under reduced pressure with the solid isolated in an argon box (0.322 g, 72%). Crystals suitable for X-ray diffraction were grown from a room-temperature solution of hexane where stirring was stopped upon PMDETA addition as orange blocks (**3a**) and yellow needles (**3b**). ^{1}H NMR (C_6D_6, 400.20 MHz): δ 1.72−1.96 (m, 23H, PMDETA) 2.37 (m, $^{3}J_{H-H}$ = 1.3 Hz, 3H, −C(Me)=), 3.20 (br-s, 1H, −C(Me)=CHH), 3.38 (d, $^{2}J_{H-P}$ = 7.65 Hz, P−CH−), 3.58 (s, 1H, −C(Me)=CHH), 7.06 (m, 2H, *p*-H), 7.19 (m, 4H, *m*-H), 7.82 (m, 4H, *o*-H). ^{7}Li NMR (C_6D_6, 155.53 MHz): δ −4.28. ^{13}C NMR (C_6D_6, 100.6 MHz): δ 25.20 (s, −C(Me)=), 44.76 (s, PMDETA), 45.86 (s, PMDETA), 53.68 (s, PMDETA), 54.87 (s, P−CH−), 57.30 (s, PMDETA), 69.43 (m, =CH_2), 126.09 (s, *p*-C), 127.72 (d, $^{3}J_{C-P}$ = 5.6 Hz, *m*-C), 132.85 (d, $^{2}J_{C-P}$ = 17.7 Hz, *o*-C), 150.21 (m, −C(Me)=), 157.59 (d, $^{1}J_{C-P}$ = 26.2 Hz, *i*-C). ^{31}P{H} NMR (C_6D_6, 162.00 MHz): δ −13.6. Due to the highly sensitive nature of this compound, satisfactory elemental analysis was not possible.

Synthesis of 4 [PhP{$CHCHCH_2Li$(TMEDA)}$_2$]. Diallylphenylphosphine (**P4**) (0.1902 g, 1.00 mmol) was dissolved in dry *n*-hexane (10 mL). *n*-Butyllithium (1.38 mL, 1.6 M in hexane, 2.2 mmol) was then added dropwise at −78 °C, forming an orange solution. After warming to room temperature and stirring for a further 2 h, TMEDA (0.33 mL, 2.2 mmol) was added dropwise with stirring, forming a dark red oil at the bottom of the flask. Solvent removal under reduced pressure formed precipitate which was isolated in an argon box (0.318 g, 73%). Crystals suitable for X-ray diffraction were grown from a concentrated solution of hexane. ^{1}H NMR (C_6D_6, 400.20 MHz): δ 1.85 (s, 8H, TMEDA−CH_2), 2.04 (s, 24H, TMEDA−CH_3), 3.16 (br-m, 4H, =CH_2), 3.62 (br-m, 2H, P−CH−), 6.95 (br-m, 2H, −CH=), 7.09 (m, 1H, *p*-H), 7.35 (m, 2H, *m*-H), 8.08 (m, 2H, *o*-H). ^{7}Li NMR (C_6D_6, 155.53 MHz): δ −5.14. ^{13}C NMR (C_6D_6, 100.6 MHz): δ 46.12 (s, TMEDA−Me), 56.55 (s, TMEDA−CH_2), 65.02 (br-m, allyl−*C*), 73.57 (br-m, allyl−*C*), 105.72 (m, =CH_2), 124.65 (br-s, *p*-C), 127.47 (d, $^{3}J_{C-P}$ = 3.9 Hz, *m*-C), 130.78 (br-d, $^{2}J_{C-P}$ = 12.9 Hz, *o*-C), 140.02 (br-m, −CH=), 151.31 (br-m, *i*-C). ^{31}P{H} NMR (C_6D_6, 162.0 MHz): δ −35.2. Due to the highly sensitive nature of this compound, satisfactory elemental analysis was not possible.

Synthesis of 5 [{$Ph_2P(O)CHC(Me)CH_2Li$(THF)}$_2$]. 2-Methylallyldiphenylphosphine oxide (**P3′**) (0.2563 g, 1.00 mmol) was loaded into a flask and suspended in dry THF (10 mL). *n*-Butyllithium (0.69 mL, 1.6 M in hexane, 1.1 mmol) was then added dropwise at −78 °C, immediately forming an orange solution. After warming to room temperature, the mixture was allowed to stir for a further 2 h. The majority of the solvent was removed under reduced pressure, and the solution was precipitated with hexane (10 mL) before being filtered. The product was further washed with hexane (2 × 10 mL), and all the remaining solvent was removed under reduced pressure. The orange solid was isolated in an argon box (0.226 g, 68%). Crystals suitable for X-ray diffraction were grown from a concentrated solution in THF layered with hexane at room temperature as orange needles. Mp (argon, sealed capillary): 130 °C. ^{1}H NMR (25 °C, THF-d_8, 400.20 MHz): δ 1.67 (br-s, 3H, −C(Me)=), 1.68 (m, 4H, THF), 2.33 (d, $^{3}J_{H-P}$ = 24.6 Hz, 1H, P−CH−), 3.14 (s, 1H, =CHH), 3.39 (d, $^{2}J_{H-H}$ = 24.6 Hz, 1H, =CHH), 3.54 (m, 4H, THF), 7.15 (m, 6H, *m* and *p*-H), 7.81 (m, 4H, *o*-H). ^{7}Li NMR (25 °C, THF-d_8, 155.53 MHz): δ −4.04, −4.50. ^{13}C NMR (25 °C, THF-d_8, 100.6 MHz): δ 26.54 (s, THF), 27.74 (d, $^{2}J_{C-P}$ = 16.8 Hz, −C(Me)=), 48.15 (d, $^{1}J_{C-P}$ = 144.0 Hz, P−CH−), 68.39 (s, THF), 82.31 (br s, =CH_2), 128.02 (d, $^{3}J_{C-P}$ = 11.0 Hz, *m*-C), 129.40 (s, *p*-C), 133.00 (d, $^{2}J_{C-P}$ = 8.9 Hz, *o*-C), 142.30 (d, $^{1}J_{C-P}$ = 105.9 Hz, *i*-C), 149.00 (br s, −C(Me)=). ^{31}P{H} NMR (25 °C, THF-d_8, 162.0 MHz): δ 26.5, 30.7, 30.9. ^{1}H NMR (100 °C, C_7D_8, 400.20 MHz): δ 1.46 (m, 4H, THF), 1.95 (br-s, 3H, −C(Me)=), 2.72 (d, $^{3}J_{H-P}$ = 24.7 Hz, $^{4}J_{H-H}$ = 1.5 Hz, 1H, P−CH−), 3.52 (m, 4H, THF), 3.57 (s, 1H, =CHH), 3.96 (s, 1H, =CHH), 7.06 (m, 2H, *p*-H), 7.06 (m, 4H, *m*-H), 7.80 (m, 4H, *o*-H). ^{7}Li NMR (25 °C, C_7D_8, 155.53 MHz): δ −3.82. ^{13}C NMR (25 °C, C_7D_8, 100.6 MHz): δ 26.03 (s, THF), 28.13 (d, $^{2}J_{C-P}$ = 17.6 Hz, −C(Me)=), 45.94 (d, $^{1}J_{C-P}$ = 133.2 Hz, P−CH−), 68.37 (s, THF), 81.62 (m, =CH_2), 128.75 (m, *p*-C), 130.75 (s, *m*-C), 132.27 (s, *o*-C), 151.78 (m, *i*-C). ^{31}P{H} NMR (25 °C, C_7D_8, 162.0 MHz): δ 36.0, 37.7. $C_{36}H_{40}Li_2O_3P_2$ (596.54): calcd (loss of one THF molecule), C 72.48, H 6.76, N 0.00. Found C 73.28, H 6.81, N 0.17. Due to the highly sensitive nature of this compound, elemental analysis within 0.4% was not attained. A difference within 0.80% in C was the closest obtained.

Synthesis of 6 [{$Ph_2P(O)CHC(Me)CH_2Li$}$_2$(TMEDA). 2-Methylallyldiphenylphosphine oxide (**P3′**) (0.2563 g, 1.00 mmol) was loaded into a flask and suspended in dry Et_2O (10 mL). *n*-Butyllithium (0.69 mL, 1.6 M in hexane, 1.1 mmol) was then added dropwise at −78 °C, immediately forming an orange solution. After warming to room temperature and stirring for a further 2 h, TMEDA (0.17 mL, 1.1 mmol) was added dropwise with stirring, turning the solution bright red. After 5 min, precipitate appeared in the mixture. The residue was extracted with hexane (10 mL) before being filtered. The solvent was removed under reduced pressure, and the dark red solid was isolated in an argon box (0.202 g, 82%). Crystals suitable for X-ray diffraction were grown from a concentrated solution in ether layered with hexane at room temperature as orange rectangular blocks. ^{1}H NMR (C_6D_6 spiked with THF-d_8, 400.20 MHz): δ 2.06 (s, 12H, TMEDA−CH_3), 2.18 (s, 4H, TMEDA−CH_2), 2.26 (s, 6H, −C(Me)=), 2.82 (d, $^{2}J_{H-P}$ = 26.5 Hz, 2H, P−CH−), 3.90 (s, 2H, −C(Me)=CHH), 4.24 (s, 2H, −C(Me)=CHH), 7.16 (m, 2H, *p*-H), 7.16 (m, 4H, *m*-H), 8.04 (m, 4H, *o*-H). ^{7}Li NMR (C_6D_6 spiked with THF-d_8, 155.53 MHz): δ −4.18. ^{13}C NMR (C_6D_6 spiked with THF-d_8, 100.6 MHz): δ 28.16 (d, $^{2}J_{C-P}$ = 17.9 Hz, −C(Me)=), 45.98 (s, TMEDA−CH_3), 46.01 (d, $^{1}J_{C-P}$ = 132.5 Hz, P−CH−), 57.84 (s, TMEDA−CH_2), 81.19 (m, =CH_2), 128.24 (m, *p*-C), 129.91 (s, *m*-C), 132.19 (d, $^{2}J_{C-P}$ = 9.5 Hz, *o*-C), 138.91 (d, $^{2}J_{C-P}$ = 104.7 Hz, −C(Me)=), 150.86 (m, *i*-C). ^{31}P{H} NMR (C_6D_6 spiked with THF-d_8, 162.0 MHz): δ 33.3. $C_{36}H_{44}Li_2N_2O_2P_2$ (612.59): calcd C 70.59, H 7.24, N 4.57. Found C 70.76, H 7.59, N 4.13. Due to the highly sensitive nature of this compound, elemental analysis within 0.4% was not attained. A difference within 0.44% in N was the closest obtained.

Synthesis of 7 [$Ph_2P(O)CHC(Me)CH_2Li$(PMDETA)]. 2-Methylallyldiphenylphosphine oxide (**P3′**) (0.2563 g, 1.00 mmol) was loaded into a flask and suspended in dry Et_2O (10 mL). *n*-Butyllithium (0.69 mL, 1.6 M in hexane, 1.1 mmol) was then added dropwise at −78 °C, immediately forming an orange solution. After warming to room temperature and stirring for a further 2 h, PMDETA (0.23 mL, 1.1 mmol) was added dropwise with stirring, turning the solution bright red. After 5 min, precipitate appeared in the mixture. The residue was extracted with hexane (10 mL) before being filtered. The solvent was removed under reduced pressure, and the dark red solid isolated in an argon box (0.270 g, 60%). Crystals suitable for X-ray diffraction were grown from a filtered concentrated solution in ether at room temperature as red columnar crystals. Mp (argon, sealed capillary): 110 °C. ^{1}H NMR (C_6D_6, 400.20 MHz): δ 1.80−

https://dx.doi.org/10.1021/acs.organomet.0c00144
Organometallics XXXX, XXX, XXX−XXX

2.20 (m, 23H, PMDETA), 2.36 (s, 3H, −C(Me)═), 3.05 (d, $^{3}J_{H-P}$ = 24.9 Hz, 1H, P−CH−), 3.96 (s, 1H, ═CHH), 4.05 (s, 1H, ═CHH), 7.13 (m, 2H, *p*-H), 7.25 (m, 4H, *m*-H), 8.32 (m, 4H, *o*-H). ^{7}Li NMR (C_6D_6, 155.53 MHz): δ −3.99. ^{13}C NMR (C_6D_6, 100.6 MHz): δ 28.31 (d, $^{2}J_{C-P}$ = 17.6 Hz, −C(Me)═), 44.15 (s, PMDETA), 45.58 (s, PMDETA), 48.52 (d, $^{1}J_{C-P}$ = 142.1 Hz, P−CH−), 53.47 (s, PMDETA), 57.20 (s, PMDETA), 81.78 (d, $^{3}J_{C-P}$ = 6.6 Hz, ═CH_2), 127.80 (m, *m*-C), 128.90 (s, *p*-C), 132.55 (d, $^{2}J_{C-P}$ = 8.7 Hz, *o*-C), 142.52 (d, $^{1}J_{C-P}$ = 105.0 Hz, −C(Me)═), 149.23 (d, $^{2}J_{C-P}$ = 7.1 Hz, *i*-C). ^{31}P{H} NMR (C_6D_6, 162.0 MHz): δ 26.1. $C_{25}H_{39}LiN_3OP$ (435.50): calcd C 68.95, H 9.03, N 9.65. Found C 68.23, H 9.00, N 9.46. Due to the highly sensitive nature of this compound, elemental analysis within 0.4% was not attained. A difference within 0.72% in C was the closest obtained.

Synthesis of 8 [$Ph_2P(O)CHCHCMe_2Li(PMDETA)$]. 3,3-Dimethylallyldiphenylphosphine oxide (**P2′**) (0.2703 g, 1.00 mmol) was loaded into a flask and suspended in dry Et2O (10 mL). *n*-Butyllithium (0.69 mL, 1.6 M in hexane, 1.1 mmol) was then added dropwise at −78 °C, forming a bright red solution. After warming to room temperature and stirring for a further 2 h, PMDETA (0.23 mL, 1.1 mmol) was added dropwise with stirring, turning the solution dark red. After 5 min, precipitate appeared in the mixture. The residue was extracted with hexane (10 mL) before being filtered. The solvent was removed under reduced pressure, and the dark red solid isolated in an argon box (0.373 g, 83%). Crystals suitable for X-ray diffraction were grown from a concentrated solution in Et_2O layered with hexane at room temperature as red needles. ^{1}H NMR (C_6D_6, 400.20 MHz): δ 1.61−2.17 (m, 23H, PMDETA), 2.17 (br-s, 6H, ═CMe_2), 3.16 (dd, $^{3}J_{H-P}$ = 20.0 Hz, J_{H-H} = 12.7 Hz, 1H, P−CH−), 6.24 (dd, $^{3}J_{H-P}$ = 13.0 Hz, J_{H-H} = 12.7 Hz, 1H, −CH═), 7.11 (m, 2H, *p*-H), 7.23 (m, 4H, *m*-H), 8.41 (m, 4H, *o*-H). ^{7}Li NMR (C_6D_6, 155.53 MHz): δ −3.94. ^{13}C NMR (C_6D_6, 100.6 MHz): δ 19.02 (s, ═CMe_2), 27.05 (s, ═CMe_2), 44.20 (s, PMDETA), 44.21 (d, $^{1}J_{C-P}$ = 147.2 Hz, P−CH−), 45.60 (s, PMDETA), 53.43 (s, PMDETA), 57.12 (s, PMDETA), 96.61 (d, $^{3}J_{C-P}$ = 21.3 Hz, ═CMe_2) 127.61 (d, $^{3}J_{C-P}$ = 10.6 Hz, *m*-C), 128.90 (s, *p*-C), 129.49 (d, $^{2}J_{C-P}$ = 9.1 Hz, −CH═), 133.41 (d, $^{2}J_{C-P}$ = 8.2 Hz, *o*-C), 142.90 (d, $^{1}J_{C-P}$ = 106.8 Hz, *i*-C). ^{31}P{H} NMR (C_6D_6, 162.0 MHz): δ 28.9. Due to the highly sensitive nature of this compound, satisfactory elemental analysis was not possible.

Synthesis of 9 [$Ph_2P(O)CHCHCH_2Li(PMDETA)$]. Allyldiphenylphosphine oxide (**P1′**) (ADPPO) (0.2423 g, 1.00 mmol) was loaded into a flask and suspended in dry Et_2O (10 mL). *n*-Butyllithium (0.69 mL, 1.6 M in hexane, 1.1 mmol) was then added dropwise at −78 °C, forming an orange solution. After warming to room temperature and stirring for a further 2 h, PMDETA (0.23 mL, 1.1 mmol) was added dropwise with stirring, turning the solution bright red. The majority of the solvent was removed under reduced pressure, and the solution was precipitated with hexane (10 mL) before being filtered. Remaining solvent was removed under reduced pressure, and the red solid isolated in an argon box (0.277 g, 66%). Crystals suitable for X-ray diffraction were grown from a concentrated solution in Et_2O layered with hexane at room temperature as red needles. ^{1}H NMR (C_6D_6, 400.20 MHz): δ 1.74−2.37 (m, 23H, PMDETA), 3.70 (dd, $^{2}J_{H-P}$ = 21.6 Hz, $^{3}J_{H-H(\beta)}$ = 12.6 Hz, 1H, P−CH−) 4.21 (dt, $^{3}J_{H-H(\beta)}$ = 9.85 Hz, $^{3}J_{H-H(trans)}$ = 3.7 Hz, 1H, −CH═CHH), 4.63 (dd, $^{3}J_{H-H(\beta)}$ = 15.89 Hz, $^{3}J_{H-H(cis)}$ = 3.3 Hz, 1H, −CH═CHH), 6.88 (tdd, $^{3}J_{H-H(trans)}$ = 15.89 Hz, $^{3}J_{H-H(\alpha)}$ = 12.63 Hz, $^{3}J_{H-H(cis)}$ = 9.85 Hz, 1H, −CH═CH_2), 7.11 (m, 2H, *p*-H), 7.23 (m, 4H, *m*-H), 8.36 (m, 4H, *o*-H). ^{7}Li NMR (C_6D_6, 155.53 MHz): δ −3.94. ^{13}C NMR (C_6D_6, 100.6 MHz): δ 44.05 (br s, PMDETA), 45.77 (s, PMDETA), 51.22 (d, $^{1}J_{C-P}$ = 146.5 Hz, P−CH−), 53.56 (s, PMDETA), 57.38 (s, PMDETA), 81.58 (d, $^{3}J_{C-P}$ = 21.8 Hz, ═CH_2), 127.71 (d, $^{3}J_{C-P}$ = 10.9 Hz, *m*-C), 129.13 (d, $^{4}J_{C-P}$ = 2.6 Hz, *p*-C), 133.30 (d, $^{2}J_{C-P}$ = 8.4 Hz, *o*-C), 141.82 (d, $^{1}J_{C-P}$ = 8.1 Hz, *i*-C), 142.06 (d, $^{2}J_{C-P}$ = 106.8 Hz, −CH═). ^{31}P{H} NMR (C_6D_6, 162.0 MHz): δ 29.2. Due to the highly sensitive nature of this compound, satisfactory elemental analysis was not possible.

Synthesis of 10 [$Ph_2PCHCHCMe_2Li(PMDETA)$]. 3,3-Dimethylallyldiphenylphosphine (**P2**) (0.2543 g, 1.00 mmol) was dissolved in dry *n*-hexane (10 mL). *n*-Butyllithium (0.69 mL, 1.6 M in hexane, 1.1 mmol) was then added dropwise at −78 °C, forming yellow solution. After warming to room temperature and stirring for a further 2 h, PMDETA (0.23 mL, 1.1 mmol) was added dropwise with stirring, turning the solution a dark orange and forming orange precipitate. The precipitate was washed with hexane (3 × 10 mL) before the remaining solvent was removed under reduced pressure with the solid isolated in an argon box (0.322 g, 72%). No crystals suitable for X-ray diffraction were acquired. ^{1}H NMR (C_6D_6, 400.20 MHz): δ 1.50−1.85 (m, 23H, PMDETA) 2.07 (m, 6H, ═CMe_2), 2.63 (dd, $^{3}J_{H-H}$ = 13.0 Hz, $^{2}J_{H-P}$ = 7.5 Hz, 1H, P−CH−), 6.37 (t, $^{3}J_{H-H}$ = 13.0 Hz, $^{3}J_{H-P}$ = 12.5 Hz, 1H, −CH═), 7.06 (m, 2H, *p*-H), 7.20 (m, 4H, *m*-H), 7.87 (m, 4H, *o*-H). ^{7}Li NMR (C_6D_6, 155.53 MHz): δ −4.50. ^{13}C NMR (C_6D_6, 100.6 MHz): δ 19.71 (d, $^{4}J_{C-P}$ = 3.1 Hz, ═CMeMe(trans)), 27.39 (d, $^{4}J_{C-P}$ = 2.6 Hz, ═CMeMe(cis)), 37.24 (br m, P−CH−), 44.55 (s, PMDETA), 45.86 (s, PMDETA), 53.48 (s, PMDETA), 57.22 (s, PMDETA), 95.94 (d, $^{3}J_{C-P}$ = 23.3 Hz, ═CMe_2), 125.93 (s, *p*-C), 127.69 (d, $^{3}J_{C-P}$ = 5.3 Hz, *m*-C), 132.87 (d, $^{2}J_{C-P}$ = 16.9 Hz, *o*-C), 136.79 (d, $^{2}J_{C-P}$ = 28.1 Hz, −CH═), 151.88 (d, $^{1}J_{C-P}$ = 19.7 Hz, *i*-C). ^{31}P{H} NMR (C_6D_6, 162.00 MHz): δ −2.5. $C_{26}H_{41}LiN_3P$ (433.55): calcd C 72.03, H 9.53, N 9.69. Found C 71.21, H 9.26, N 9.41. Due to the highly sensitive nature of this compound, elemental analysis within 0.4% was not attained. A difference within 0.82% in C was the closest obtained.

Synthesis of 11 [$Ph_2PCHC(Me)CH_2Li(TMEDA)$]. 2-Methylallyldiphenylphosphine (**P3**) (0.2403 g, 1.00 mmol) was dissolved in dry *n*-hexane (10 mL). *n*-Butyllithium (0.69 mL, 1.6 M in hexane, 1.1 mmol) was then added dropwise at −78 °C, forming a slightly yellow solution with a small amount of yellow precipitate. After warming to room temperature and stirring for a further 2 h, TMEDA (0.17 mL, 1.1 mmol) was added dropwise with stirring, turning the solution orange and forming yellow precipitate. The precipitate was washed with hexane (3 × 10 mL) before the remaining solvent was removed under reduced pressure with the solid isolated in an argon box (0.254 g, 70%). No crystals suitable for X-ray diffraction were acquired. ^{1}H NMR (C_6D_6, 400.20 MHz): δ 1.56 (br-s, 4H, TMEDA−CH_2), 1.73 (br-s, 12H, TMEDA−CH_3), 2.34 (br-s, 3H, −C(Me)═), 3.27 (br-s, 1H, −C(Me)═CHH), 3.34 (br-s, 1H, −C(Me)═CHH), 3.55 (br-s, 1H, P−CH−), 7.08 (m, 2H, *p*-H), 7.20 (m, 4H, *m*-H), 7.82 (m, 4H, *o*-H). ^{7}Li NMR (C_6D_6, 155.53 MHz): δ −4.47. ^{13}C NMR (C_6D_6, 100.6 MHz): δ 23.06 (br-m, −C(Me)═), 45.71 (s, TMEDA−CH_3), 55.02 (br-m, ═CH_2), 56.45 (s, TMEDA−CH_2), 67.37 (br-m, P−CH−), 126.52 (br-s, *p*-C), 128.00 (m, *m*-C), 132.66 (br-s, *o*-C), 150.01 (br-m, −C(Me)═), 157.43 (br-m, *i*-C). ^{31}P{H} NMR (C_6D_6, 162.00 MHz): δ −32.7, −27.6, −19.7. ^{1}H NMR (THF-d_8, 400.20 MHz): δ 1.93 (s, 3H, −C(Me)═), 2.15 (s, 12H, TMEDA−CH_3), 2.31 (s, 4H, TMEDA−CH_2), 2.73 (br-s, 1H, ═CHH), 2.97 (br-s, 1H, P−CH−), 3.18 (br-s, 1H═CHH), 7.00 (m, 2H, *p*-H), 7.09 (m, 4H, *m*-H), 7.36 (m, 4H, *o*-H). ^{7}Li NMR (THF-d_8, 155.53 MHz): δ −6.82. ^{13}C NMR (THF-d_8, 100.6 MHz): δ 24.55 (br-m, −C(Me)═), 46.31 (s, TMEDA−CH_3), 56.53 (br-m, P−CH−), 58.91 (s, TMEDA−CH_2), 67.13 (br-m, ═CH_2), 126.21 (s, *p*-C), 127.86 (d, $^{3}J_{C-P}$ = 5.6 Hz, *m*-C), 132.82 (d, $^{2}J_{C-P}$ = 18.0 Hz, *o*-C), 150.16 (br-m, *i*-C), 158.24 (d, $^{2}J_{C-P}$ = 29.1 Hz, −C(Me)═). ^{31}P{H} NMR (THF-d_8, 162.00 MHz): δ −17.4. Due to the highly sensitive nature of this compound, satisfactory elemental analysis was not possible.

Synthesis of 12 [$Ph_2P(O)CHCHCH_2Li{\cdot}Et_2O$]. Allyldiphenylphosphine oxide (**P1′**) (0.2423 g, 1.00 mmol) was loaded into a flask and suspended in dry Et_2O (10 mL). *n*-Butyllithium (0.69 mL, 1.6 M in hexane, 1.1 mmol) was then added dropwise at −78 °C, forming an orange solution. After warming to room temperature, it was allowed to stir for a further 2 h. The majority of the solvent was removed under reduced pressure, and the solution was precipitated with hexane (10 mL) before the supernatant was filtered off. Remaining solvent was removed under reduced pressure, and the red solid was isolated in an argon box (0.130 g, 42%). No crystals suitable for X-ray diffraction were acquired. ^{1}H NMR (C_6D_6, 400.20 MHz): δ 1.06 (br-t, 6H, Et_2O−CH_3), 3.22 (br-q, 4H, Et_2O−CH_2), 3.37 (dd, $^{2}J_{H-P}$ = 21.0 Hz,

https://dx.doi.org/10.1021/acs.organomet.0c00144
Organometallics XXXX, XXX, XXX−XXX

$^{3}J_{H-H(\beta)}$ = 12.3 Hz, 2H, P−CH−) 3.66 (dt, $^{3}J_{H-H(\beta)}$ = 10.1 Hz, $^{3}J_{H-H(trans)}$ = 3.5 Hz, 2H, =CHH(cis)), 4.17 (dd, $^{3}J_{H-H(\beta)}$ = 16.4 Hz, $^{3}J_{H-H(cis)}$ = 2.6 Hz, 2H, =CHH(trans)), 6.63 (dddd, $^{3}J_{H-P}$= 18.1 Hz, $^{3}J_{H-H(trans)}$ = 16.5 Hz, $^{3}J_{H-H(\alpha)}$ = 12.3 Hz, $^{3}J_{H-H(cis)}$ = 10.1 Hz, 2H, −CH=), 7.03 (m, 4H, *p*-H), 7.03 (m, 2H, *p*-H), 7.03 (m, 4H, *m*-H), 7.91 (m, 4H, *o*-H). ^{7}Li NMR (C_6D_6, 155.5 MHz): δ −3.67. ^{13}C NMR (C_6D_6, 100.6 MHz): δ 15.54 (s, Et_2O-CH_3), 46.49 (br-m, P−CH−), 65.90 (s, Et_2O-CH_2), 83.66 (br-m, $=CH_2$), 128.68 (d, $^{3}J_{C-P}$ = 11.6 Hz, *m*-C), 130.84 (d, $^{4}J_{C-P}$ = 2.3 Hz, *p*-C), 133.32 (d, $^{2}J_{C-P}$ = 9.8 Hz, *o*-C), 141.82 (br m, −CH=). ^{31}P{H} NMR (C_6D_6, 162.0 MHz): δ 38.8. Due to the highly sensitive nature of this compound, satisfactory elemental analysis was not possible.

■ ASSOCIATED CONTENT

Supporting Information

The Supporting Information is available free of charge at https://pubs.acs.org/doi/10.1021/acs.organomet.0c00144.

Summary of crystallographic data for complexes **1**−**9** and **P1′**−**4′**, NMR spectroscopy data for compounds **1**−**12** (PDF)

Coordinates of **3a** and **3b** (XYZ)

Accession Codes

CCDC 1953194−1953207 contain the supplementary crystallographic data for this paper. These data can be obtained free of charge via www.ccdc.cam.ac.uk/data_request/cif, or by emailing data_request@ccdc.cam.ac.uk, or by contacting The Cambridge Crystallographic Data Centre, 12 Union Road, Cambridge CB2 1EZ, UK; fax: +44 1223 336033.

■ AUTHOR INFORMATION

Corresponding Author

Victoria L. Blair − *School of Chemistry, Monash University, Melbourne, Victoria 3800, Australia;* orcid.org/0000-0002-2984-6048; Email: Victoria.blair@monash.edu

Authors

Nimrod M. Eren − *School of Chemistry, Monash University, Melbourne, Victoria 3800, Australia*

Samantha A. Orr − *School of Chemistry, Monash University, Melbourne, Victoria 3800, Australia*

Christopher D. Thompson − *School of Chemistry, Monash University, Melbourne, Victoria 3800, Australia;* orcid.org/0000-0001-6913-9922

Emily C. Border − *School of Chemistry, Monash University, Melbourne, Victoria 3800, Australia*

Michael A. Stevens − *School of Chemistry, Monash University, Melbourne, Victoria 3800, Australia*

Complete contact information is available at: https://pubs.acs.org/10.1021/acs.organomet.0c00144

Notes

The authors declare no competing financial interest.

■ ACKNOWLEDGMENTS

We thank the Australian Research Council (DP170104722) and Monash University for financial support of this work. This research was undertaken in part using the MX1 beamline at the Australian Synchrotron, part of ANSTO. We acknowledge help provided by Dr. Craig Forsyth and Dr. Peter Nicholls of the Monash X-ray and NMR platforms.

■ REFERENCES

(1) Lappert, M.; Protchenko, A.; Power, P.; Seeber, A. *Metal Amide Chemistry*; Wiley, 2008.

(2) Wauters, I.; Debrouwer, W.; Stevens, C. V. Preparation of Phosphines through C-P Bond Formation. *Beilstein J. Org. Chem.* **2014**, *10*, 1064−1096.

(3) Arrechea, P. L.; Buchwald, S. L. Biaryl Phosphine Based Pd(II) Amido Complexes: The Effect of Ligand Structure on Reductive Elimination. *J. Am. Chem. Soc.* **2016**, *138* (38), 12486−12493.

(4) Noyori, R. Asymmetric Catalysis: Science and Opportunities (Nobel Lecture). *Angew. Chem., Int. Ed.* **2002**, *41* (12), 2008−2022.

(5) Guo, H.; Fan, Y. C.; Sun, Z.; Wu, Y.; Kwon, O. Phosphine Organocatalysis. *Chem. Rev.* **2018**, *118* (20), 10049−10293.

(6) Shameem, M. A.; Orthaber, A. Organophosphorus Compounds in Organic Electronics. *Chem. - Eur. J.* **2016**, *22* (31), 10718−10735.

(7) Demkowicz, S.; Rachon, J.; Daśko, M.; Kozak, W. Selected Organophosphorus Compounds with Biological Activity. *RSC Adv.* **2016**, *6* (9), 7101−7112.

(8) Huang, W. S.; Liu, S.; Zou, D.; Thomas, M.; Wang, Y.; Zhou, T.; Romero, J.; Kohlmann, A.; Li, F.; Qi, J.; et al. Discovery of Brigatinib (AP26113), a Phosphine Oxide-Containing, Potent, Orally Active Inhibitor of Anaplastic Lymphoma Kinase. *J. Med. Chem.* **2016**, *59* (10), 4948−4964.

(9) Stockland, R. A. Synthesis of Organophosphines, Phosphonates, and Related Compounds. *Practical Functional Group Synthesis* **2016**, 219−470.

(10) Musina, E. I.; Balueva, A. S.; Karasik, A. A. Phosphines: Preparation, Reactivity and Applications. *Organophosphorus Chem.* **2019**, *48*, 1−63.

(11) Andrews, P. C.; Blair, V. L.; Koutsaplis, M.; Thompson, C. D. Anion Rearrangements of Alkali Metal Complexes of the Chiral Amine (S)- N -α-(Methylbenzyl)Phenylallylamine: Structural and Solution Insights. *Organometallics* **2012**, *31* (23), 8135−8144.

(12) Border, E. C.; Koutsaplis, M.; Andrews, P. C. The Strange Case of Sodium (S)-N-α-(Methylbenzyl)Allylamide: Anion Rearrangement, Decomposition, and a Peculiar Propyl Addition. *Organometallics* **2016**, *35* (3), 303−305.

(13) Flynn, M. T.; Stott, R.; Blair, V. L.; Andrews, P. C. Loss of Chirality through Facile Lewis Base Mediated Aza-Enolate Formation in Na and K (S)-N-(α-Methylbenzyl)Methallylamides. *Organometallics* **2016**, *35* (16), 2707−2714.

(14) Davies, S. G.; Smith, A. D.; Price, P. D. The Conjugate Addition of Enantiomerically Pure Lithium Amides as Homochiral Ammonia Equivalents: Scope, Limitations and Synthetic Applications. *Tetrahedron: Asymmetry* **2005**, *16* (17), 2833−2891.

(15) Whisler, M. C.; Beak, P. Synthetic Applications of Lithiated N-Boc Allylic Amines as Asymmetric Homoenolate Equivalents. *J. Org. Chem.* **2003**, *68* (4), 1207−1215.

(16) Laffoon, S. D.; Wu, Z.; Hull, K. L. Rhodium-Catalyzed Asymmetric Synthesis of β-Branched Esters from Allylic Amines. *Chem. Commun.* **2018**, *54* (56), 7814−7817.

(17) Vanable, E. P.; Kennemur, J. L.; Joyce, L. A.; Ruck, R. T.; Schultz, D. M.; Hull, K. L. Rhodium-Catalyzed Asymmetric Hydroamination of Allyl Amines. *J. Am. Chem. Soc.* **2019**, *141* (2), 739−742.

(18) Skoda, E. M.; Davis, G. C.; Wipf, P. Allylic Amines as Key Building Blocks in the Synthesis of (E)-Alkene Peptide Isosteres. *Org. Process Res. Dev.* **2012**, *16*, 26−34.

(19) Stephan, D. W.; Erker, G. Frustrated Lewis Pairs: Metal-Free Hydrogen Activation and More. *Angew. Chem., Int. Ed.* **2010**, *49* (1), 46−76.

(20) Thapper, A.; Sparr, E.; Johnson, B. F. G.; Lewis, J.; Raithby, P. R.; Nordlander, E. Reversible π-Coordination of Triallylphosphine in a Trinuclear Ruthenium Carbonyl Cluster. *Inorg. Chem. Commun.* **2004**, *7* (3), 443−446.

(21) Pomogailo, S. I.; Chuev, I. I.; Dzhardimalieva, G. I.; Yarmolenko, A. V.; Makhaev, V. D.; Aldoshin, S. M.; Pomogailo, A. D. Synthesis and Reactivity of Metal-Containing Monomers 51. Synthesis and Molecular Structure of the Cluster-Containing

Complex [Rh 6 (CO) 14 (μ,η,2-$PPh_2CH_2CH{=}CH_2$)]. *Russ. Chem. Bull.* **1999**, *48* (6), 1174−1177.
(22) Appel, R.; Loos, R.; Mayr, H. Nucleophilicity Parameters for Phosphoryl-Stabilized Carbanions and Phosphorus Ylides: Implications for Wittig and Related Olefination Reactions. *J. Am. Chem. Soc.* **2009**, *131* (2), 704−714.
(23) Clayden, J.; Warren, S. Stereocontrol in Organic Synthesis Using the Diphenylphosphoryl Group. *Angew. Chem., Int. Ed. Engl.* **1996**, *35*, 241−270.
(24) Larsen, R. O.; Aksnes, G. The Effect of the Phosphoryl Substituents on the Stereochemistry of the Horner Reaction. *Phosphorus Sulfur Relat. Elem.* **1983**, *16* (3), 339−344.
(25) Grayson, J. I.; Norrish, H. K.; Warren, S. Synthesis of Phosphindoline Oxides, Tetrahydrophosphinoline Oxides, and Related Compounds by Cyclisation of Allyl- and Vinyl-Phosphine Oxides. *J. Chem. Soc., Perkin Trans. 1* **1976**, *23*, 2556−2562.
(26) Armstrong, S. K.; Warren, S.; Collington, E. W.; Naylor, A. Stereocontrolled Synthesis of Homoallylic Amines Using Phosphine Oxides and Isoxazolines. *Tetrahedron Lett.* **1991**, *32* (33), 4171−4174.
(27) Ukai, J.; Ikeda, Y.; Ikeda, N.; Yamamoto, H. Direct, Stereoselective Synthesis of Either E- or Z-1,3-Dienes. *Tetrahedron Lett.* **1983**, *24* (37), 4029−4032.
(28) Ikeda, Y.; Ukai, J.; Ikeda, N.; Yamamoto, H. Stereoselective Synthesis of (z)- and (e)-1,3-Alkadienes from Aldehydes Using Organotitanium and Lithium Reagents. *Tetrahedron* **1987**, *43* (4), 723−730.
(29) Beddoe, R. H.; Andrews, K. G.; Magné, V.; Cuthbertson, J. D.; Saska, J.; Shannon-Little, A. L.; Shanahan, S. E.; Sneddon, H. F.; Denton, R. M. Redox-Neutral Organocatalytic Mitsunobu Reactions. *Science* **2019**, *365* (6456), 910−914.
(30) Blair, V. L.; Stevens, M. A.; Thompson, C. D. The Importance of the Lewis Base in Lithium Mediated Metallation and Bond Cleavage Reaction of Allyl Amines and Allyl Phosphines. *Chem. Commun.* **2016**, *52* (52), 8111−8114.
(31) Blaurock, S.; Kühl, O.; Hey-Hawkins, E. Lithio-(Diphenylphosphino)Methane−Tetramethylethylenediamine: It's a Dimer! *Organometallics* **1997**, *16* (4), 807−808.
(32) Andrews, P. C.; Blair, V. L.; Border, E. C.; Peatt, A. C.; Maclellan, J. G.; Thompson, C. D. Alkali-Metal-Induced C-C Bond Cleavage and CH_4 Elimination in the Amido → Aza-Allyl Transformation of the (S)- N -α-(Methylbenzyl) Benzylamido Anion. *Organometallics* **2013**, *32* (24), 7509−7519.
(33) Andrews, P. C.; Koutsaplis, M.; Robertson, E. G. Thermodynamically Favored Anion Rearrangements in Li and Na Complexes of (S)-N-α-(Methylbenzyl)Allylamine. *Organometallics* **2009**, *28* (6), 1697−1704.
(34) Tang, S.; Zhang, X.; Sun, J.; Niu, D.; Chruma, J. J. 2-Azaallyl Anions, 2-Azaallyl Cations, 2-Azaallyl Radicals, and Azomethine Ylides. *Chem. Rev.* **2018**, *118* (20), 10393−10457.
(35) Frisch, M. J. G.; Trucks, W.; Schlegel, H. B.; Scuseria, G. E.; Robb, M. A.; Cheeseman, J. R.; Scalmani, G.; Barone, V.; Mennucci, B.; Petersson, G. A.; et al. *Gaussian 16, Rev. D.01*; 2016.
(36) Al-Masri, H.; Sieler, J.; Hey-Hawkins, E. Synthesis and Characterization of Novel Chelated Dimethylamino Lithium Alkoxides: Molecular Structures of $[1\text{-}LiOC(C_6H_{11})_2\text{-}2\text{-}NMe_2C_6H_4]_2$ and $[1\text{-}LiOCPh_2CH_2\text{-}2\text{-}NMe_2C_6H_4]_2$. *Appl. Organomet. Chem.* **2003**, *17* (1), 63−67.
(37) Reisinger, A.; Trapp, N.; Krossing, I. AgOC(CF3)3: Synthesis and Applications of the First Donor-Free Silver(I) Alkoxide. *Organometallics* **2007**, *26* (8), 2096−2105.
(38) Clegg, W.; Liddle, S. T.; Davies, R. P.; Dunbar, L.; Feeder, N.; Snaith, R.; Wheatley, A. E. H.; Mulvey, R. E. Lithiated Organophosphorus Enamines: A New Synthetic Approach and the First Crystal Structures. *Chem. Commun.* **1999**, *15*, 1401−1402.
(39) *US, B. A. M. V2012.2.0*; Bruker Apex. 2006.
(40) Sheldrick, G. M. *SADABS v2.30.*; Univ. Gottingen 2002.
(41) Cowieson, N. P.; Aragao, D.; Clift, M.; Ericsson, D. J.; Gee, C.; Harrop, S. J.; Mudie, N.; Panjikar, S.; Price, J. R.; Riboldi-Tunnicliffe, A.; et al. MX1: A Bending-Magnet Crystallography Beamline Serving Both Chemical and Macromolecular Crystallography Communities at the Australian Synchrotron. *J. Synchrotron Radiat.* **2015**, *22* (1), 187−190.
(42) Sheldrick, G. M. SHELXT - Integrated Space-Group and Crystal-Structure Determination. *Acta Crystallogr., Sect. A: Found. Adv.* **2015**, *71* (1), 3−8.
(43) Sheldrick, G. M. Crystal Structure Refinement with SHELXL. *Acta Crystallogr., Sect. C: Struct. Chem.* **2015**, *71*, 3−8.

https://dx.doi.org/10.1021/acs.organomet.0c00144
Organometallics XXXX, XXX, XXX−XXX